



Characterization of the soil and rock hosting an aquifer with possible uses for drinking water and irrigation in SE Panama City using Geotechnical, Geophysical and Geochemical parameters

Ana Cristina González-Valoys^{1,2,3} · Miguel Vargas-Lombardo^{4,5} · Raimundo Jiménez-Ballesta³ · Jonatha Arrocha¹ · Eric Gutiérrez⁶ · Efrén García-Ordiales⁷ · Pablo Cienfuegos⁷ · Francisco Jesús García-Navarro⁸ · Pablo Higuera²

Received: 1 June 2021 / Accepted: 15 April 2022 / Published online: 7 May 2022
© The Author(s) 2022

Abstract

The supply of water to populations is a basic need that has been threatened more frequently in recent years due to climate change, which renders seeking other sources of water essential. The hydrochemistry of the groundwater of the aquifer located in the UTP Tocumen was characterized by previous research to determine its possible use as a source of drinking water and irrigation water. The objective of this study is to characterize the soil and rock hosting the aquifer to acquire more information about them with a view to possibly exploit an alternative source of drinking water. To this end, a 10-m-depth survey was conducted to obtain soil and rock samples from the area, and to characterize geotechnical and geochemical parameters. 2D electrical resistivity tomography was used to create a lithological model of the aquifer and to correlate the data. Soil is residual of the technosol type, considered permeable with a transmissivity level that favors rainwater infiltration, followed by the soil–rock interface, where rock is weathered. It's followed by a sedimentary rock corresponding to marly siltstones with a certain degree of tectonic fractures that allow water infiltration and its accumulation in the rocks, constituting the aquifer. The 2D electrical resistivity suggests two water accumulations: a superficial and a deep one. There was a good correlation between the aquifer water's chemistry and the rock geochemistry.

Keywords Aquifer · Marlstone · Electrical resistivity · Groundwater · Tocumen

✉ Ana Cristina González-Valoys
ana.gonzalez1@utp.ac.pa

¹ Centro Experimental de Ingeniería, Universidad Tecnológica de Panamá, Vía Tocumen, 0819-07289 Panama City, Panama

² Instituto de Geología Aplicada, Universidad de Castilla-La Mancha, EIMI Almadén, Plaza Manuel Meca 1, Almadén, 13400 Ciudad Real, Spain

³ Departamento de Geología y Geoquímica, Universidad Autónoma de Madrid, Ciudad Universitaria de Cantoblanco, 28049 Madrid, Spain

⁴ Facultad de Ingeniería de Sistemas Computacionales, Universidad Tecnológica de Panamá, Campus Universitario Dr. Víctor Levi Sasso, Ricardo J. Alfaro Avenue, 0819-07289 Panama City, Panama

⁵ SNI-SENACYT Sistema Nacional de Investigación-Secretaría Nacional de Ciencia, Tecnología E Innovación, Clayton, Ciudad del Saber Edif.205, 0816-02852 Panama City, Panama

⁶ Departamento de Geotecnia, Facultad de Ingeniería Civil, Universidad Tecnológica de Panamá, Campus Universitario Dr. Víctor Levi Sasso, Ricardo J. Alfaro Avenue, 0819-07289 Panama City, Panama

⁷ Departamento de Explotación y Prospección de Minas, Universidad de Oviedo, Independencia Street, 13, 33004 Oviedo, Spain

⁸ Escuela Técnica Superior de Ingenieros Agrónomos de Ciudad Real, Universidad de Castilla-La Mancha, Ronda de Calatrava nº 7, 13071 Ciudad Real, Spain

Introduction

Water is a prime resource needed for human consumption, agriculture, livestock and industry that comes in increasingly short supply. Tropical countries with high to very high pluviosity traditionally have an adequate amount of rainfall. However, two aspects typically affect this situation: first, irregular rain distribution, with heavy storm episodes that are difficult to control in water storage terms; second, lack of adequate infrastructure to collect and store the enormous amounts of water deposited during such events. This is the case of Panama City, the capital of the Republic of Panama.

Panama City, with a population of 880,691 (Contraloría General de la República de Panamá 2010), is located on the Pacific Ocean coast. According to the Köppen climate classification April (Dirección de Hidrometeorología de ETESA 2007), Panama City has a tropical savanna climate (Köppen Aw), which is slightly drier than a tropical monsoon climate. The average annual precipitation is 1900 mm (74.8 in). The wet season is from May to December, and the dry season from January to April (Dirección de Hidrometeorología de ETESA 2007). Throughout the year, temperatures average around 27 °C (81°F) (<https://web.archive.org/web/20080630020659/http://wwis.inm.es/076/c01221.htm>).

Furthermore, flooding events like those which occurred in December 2010 (the so-called “Storm of the Purísima”), lead to torrential rains that increase the turbidity of reservoir lakes and disable the drinking water production in water treatment plants, and sometimes occur in this region. It took almost 3 months to solve this problem and, thus, left Panama City without this vital liquid (La Estrella de Panama 2012). Moreover, climate change has caused drought periods for some years that have threatened the water supply and the transit of ships through the Panama Canal (El País 2020; Diario Las Américas 2020). In light of this, groundwater could be an appropriate water supply alternative during such catastrophic events, or during possible drought periods.

The present study intends to obtain a better understanding of the nature of the groundwater stored in the Tocumen sector, located to the ENE of the town center (González-Valoys et al. 2021). We extended our previous research work to study the host soil and rocks to understand the relation between water and its hosts based on the site’s geophysical properties (electric resistivity), and the geotechnical parameters of soil and rock, the physicochemical and geochemical parameters of soil and rock, and the chemical composition of the water contained therein (De Caro et al. 2017; Shomar 2015). This synergic combination of techniques was expected to provide reliable information to assess the possibilities of this aquifer being used as a reliable water supply (Abdel-Satar et al. 2017; Armengol et al. 2017; Chidya et al. 2015; Zhang et al. 2018).

The study area is located close to both the urban area and the Pacific coast, where human and industrial activities are conducted that may negatively impact the aquifer (Appelo and Postma 2004; Bakhshipour et al. 2016; Jordanova et al. 2013).

Materials and methods

Study area

The study site is located at latitude 9° 3′ 57.93″ N and longitude 79° 24′ 23.22″ W in the southeast coastal area of the Isthmus of Panama (Fig. 1). The Tocumen sector of Panama City corresponds to an industrial and residential sector, where part of the Technological University of Panama is located and constitutes the ENE outskirts of the city. Its topography is almost plain, with marshes and mangroves extending from the site to the coast (~5000 m).

The area has a characteristic tropical climate (Awi type, savanna tropical climate) according to the Köppen climate classification map, with annual rainfall > 1000 mm (Dirección de Hidrometeorología de ETESA 2007). Figure 2 shows the climograph with ETESA meteorological station data from 2012 to 2020 (Dirección de Hidrometeorología de ETESA 2021). We can see that the dry season includes the months of January to March (lowest rainfall) and the rainy season goes from April to December, when the rainiest months are October and November. Regarding the environmental temperature, the highest temperatures occur in dry months.

The geology of the area includes marine sedimentary rocks that correspond to the Panama Formation from the Tertiary age. It consists mainly of tuffaceous sandstones, tuffaceous shales and limestones (Guardia 2018). The petrographic analysis of the rock in this area shows that it is comprised of marly siltstone (marl), with a clastic structure and a uniform texture, formed from silt-sized fragments of micrite, shells and microfossil fragments (microforaminifers) with abundant chloritic–clayey material, sporadic fragments of silicates (including quartz, and especially feldspars, rare Fe–Mg minerals), some traces of carbonous material and very rare magnetite (Gutiérrez 2021).

A shallow water well (24 m deep) is sporadically used for water production by means of a small pump (1.5 Hp), which was installed at the site in 1993 (Vega 2004). A preliminary test determined that at a pumping flow of 2.52 L/s, the well’s efficiency (UTP-ET) was 87.9%. The Cooper & Jacob Method (Kruseman et al. 1970) gave a preliminary transmissivity (T) value of 21.1 m²/day, and a storage coefficient (S) of 2.08×10^{-3} was obtained by the Theis Method (Kruseman et al. 1970). Given this S value, the aquifer is semiconfined and presents vertical percolation according to



Fig. 1 Study area location map

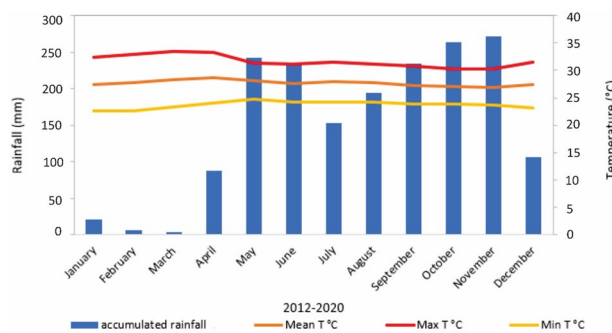


Fig. 2 Climograph: Tocumen weather station 2012–2020

the Abatement vs. Time curve (Vega 2004). A pumping test run at constant flow for 72 h in October 2015 determined that 100% efficiency is obtained at a flow of 1.26 L/s, and the well stabilizes at 6.15 m (Alpirez et al. 2015). The hydraulic gradient is relatively low with a value of 6.10×10^{-4} . Given that the area is flat with only a slight slope, the flow direction is south to north (Alpirez et al. 2015).

The aquifer’s recharge is very important (Abiyi et al. 2018; Barbera et al. 2018; Healy and Cook 2002; Martínez et al. 2017). Figure 3 shows the graph of the temporal

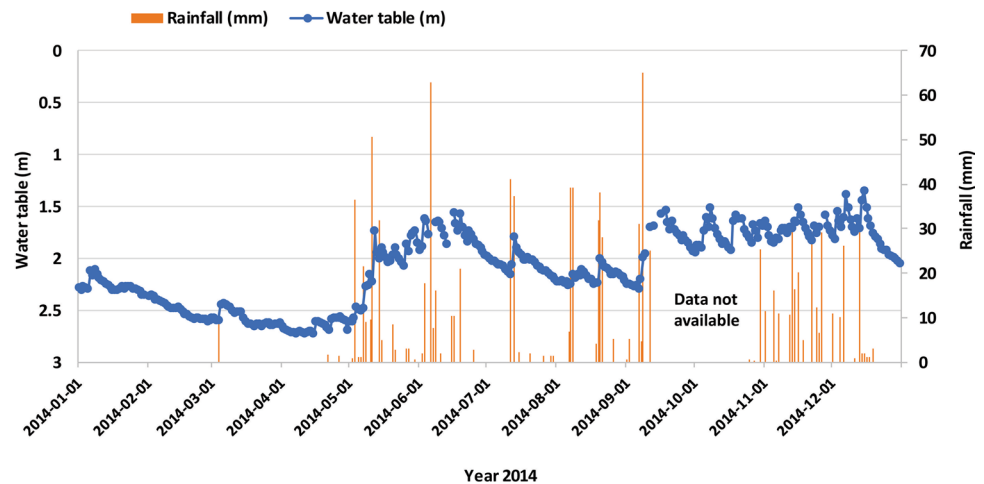
evolution of the watertable in the studied well (Centro de Investigaciones Hidráulicas e Hidrotécnicas 2016) vs. rainfall (Dirección de Hidrometeorología de ETESA 2021) for 2014, which shows that the rainfall in the area directly influences the watertable in the well, because in dry months, the water level lowers when rain is absent. The much higher rainfall that falls during the rainy season rapidly produces a net recharge of the water level in the well.

Methodology

Fieldwork was carried out between June and August 2015 during the rainy season. Laboratory studies were conducted at the Experimental Engineering Center (CEI) of the Technological University of Panama.

The methodology herein applied is based on several complementary techniques: a 10-m-deep well was drilled in the area to allow the soil and rock to be sampled and characterized using physicochemical and geotechnical parameters, as well as a chemical analysis. In addition, geophysics employed with 2D electrical resistivity tomography (ERT) (Mojica et al. 2013; Ho et al. 2017; Benabdelouahab et al. 2018) provided a basic scenario of the lithologies in the area

Fig. 3 Temporal evolution of the water table vs. rainfall 2014



and allowed a lateral interpretative extension of the data provided by the section obtained in the well.

The Geotechnical Laboratory (LABGEO) of the Technological University of Panama drilled a 10-m-deep well with a diameter of 75.7 mm in the area adjacent to the water extraction well (24 m deep), where the hydrogeochemical study was carried out (Fig. 4a). Drilling was performed using a rotary diamond drilling machine (Acker, model AD-II) with a double-tube recovery system. The watertable was detected at a depth of 2.50 m 24 h after drilling ended (Arrocha 2015). During drilling, the Rock Quality Designation (RQD) parameter was estimated. This parameter indicates the degree of jointing or fracture in a rock mass measured as a percentage, where an RQD of 75% or more shows good quality hard rock and one less than 50% denotes low quality weathered rock (The Constructor 2018).

In parallel, the Engineering and Applied Sciences Research Laboratory (LIICA) of the Technological University of Panama performed a 2D electrical resistivity tomography over a 40-m length using a Syscal R1 resistivity meter (<http://www.iris-instruments.com/syscal-r1plus.html>) with a multicable system powered by a 12 V battery. Forty-one electrodes were employed with a 1-m separation, whose Wenner–Schlumberger configuration allowed good resolution tomography to be obtained at a depth of 8 m. Data was processed using the EarthImager 2D software (<https://www.agiusa.com/agi-earthimager-2d>) and exported to Surfer 12 (<https://www.goldensoftware.com/products/surfer>) for representation purposes (Mojica 2015).

Four samples were taken from the drill's profile, corresponding to the different lithologies observed on it (Table 1; Fig. 4). The samples corresponding to complete soil and to fragments of underlying rock were taken using gloves, stored in plastic bags and kept at room temperature until analysis.

Sample preparation included sieving the soil sample to separate the > 2 mm fraction. Rock fragments were crushed and then also sieved to < 2 mm. The samples for the

geochemical analyses were prepared by CEMEX, including grinding to < 100 μm .

The physicochemical parameters were determined by the Industrial Analysis and Environmental Sciences Laboratory (LABAICA). The applied methodologies included: ASTM D 4972 (for pH and EC) in a 1:5 suspension (w/V) using a multiparameter benchtop Orion Versa Star Pro device; ASTM D 2974 for organic matter content by weight loss at 455 °C; cationic exchange capacity (CEC) by the potentiometer method (Weaver et al. 1991); calcium carbonate determination according to Skinner and Halstead (1958); sulfate determination based on ASTM D1580 (ASTM 2004); chloride determination as per AASTHO T-291 (2013). The geochemical analyses included SiO_2 , Al_2O_3 , Fe_2O_3 , CaO , MgO , SO_3 , Na_2O and K_2O , and were carried by CEMEX Panama following the X-ray fluorescence technique.

Non organic soil (Sample-2) was also characterized by determining the Atterberg limit (ASTM D4318), and granulometry (ASTM C6913) by a texture classification according to the Unified Soil Classification System (USCS) (ASTM D 2487) (ASTM 2004).

Mechanical unweathered rock behavior (three subsamples from sample 4) was established by axial compression testing (ASTM D 7012) (ASTM 2004) using an ELE International device (model ACCU-TEK 350 digital series).

Results

Geotechnical tests

The geotechnical parameters (Table 2) indicated that soil (Sample-2) corresponded to the GC group (clay gravel with sand), according to the results obtained from the grain size and the Atterberg limits for the USCS (Unified Soil Classification System).

Fig. 4 Study area: (a) drilling of well; (b) lithological logs of drill cores. The different lithological sections described in the location of the three subsamples 4 are indicated



Table 1 Identification of samples

Identification	Lithological section	Depth (m)	Lithology (visual description)
Sample 1	Section #1	0.00–0.10	Topsoil, brown. Organic layer, including vegetation waste
Sample 2	Section #2	0.10–1.00	Brown soil. Soil, constituted by clayey gravel with sand
Sample 3	Section #3	1.00–2.90	Light brown rock, weathered. Sedimentary, weathered rock, very poor quality, light brown in color
Sample 4	Section #4	2.90–10.00	Light gray rock, unweathered, healthy. Sedimentary rock with moderately soft hardness (RH-2), weak resistance, of regular to excellent quality, and light gray in color

The results of the axial compression test carried out on three subsamples of sample 4 (4-1, 4-2, 4-3) are presented in Table 3. These values can be considered normal for lutitic rocks (Kiamco et al. 2004). As well, the results of the visual inspection of discontinuities observed in the rock within the interval 2.9 to 10 m (samples 3 and 4) are presented in Table 4. Figure 5 shows the drilling profile

at a 10-m depth and indicates the parameters estimated by visual inspection.

Electrical resistivity tomography

This technique is widely used in hydrogeological studies, because it allows the possible presence of groundwater to

Table 2 Classification (granulometric analysis and consistency limits)

Hole	Sample-2
Sampling depth (m)	0.10–1.00
USCS classification	GC
Description	Clay gravel with sand
Color	Light brown
Liquid limit, LL	61
Plastic limit, PL	26
Plasticity index, PI	35

be detected from the interpretation of resistivity images, as well as an interpretation of the site's stratigraphy, without having to drill; that is, non-invasively (Kumar et al. 2016, Wahab et al. 2021). The employed electronic configuration corresponds to an arrangement of the Wenner–Schlumberger type, which allows the structure to be visualized laterally and in depth, with good resolution and depth for research in the study area. The 2D electrical resistivity tomography had 19 depth levels and 380 apparent resistivity values and thus provided a distribution section of the measured data. This representation is the result of the inversion that provides a distribution of the electrical resistivity of subsoil at a real depth (8 m) (Mojica 2015).

The 2D tomography study suggests the presence of groundwater, which coincided with the limit between the weathered and unweathered rocks (Mojica et al. 2012; Mojica 2018), as shown in Figs. 6 and 7. The smooth inversion method (see Fig. 6) included three iterations and an RMS calculation error of 2.58%. The robust inversion method (Fig. 7) involved three iterations and an RMS calculation error of 2.83% (Mojica 2015). Although the error in the robust inversion was slightly larger than that for the soft

one, both figures basically showed the same calculated electrical resistivity profile for the terrain. Both figures show the inversion profile in comparison to the drilling profile. The calculated electrical resistivity tomography corresponded very well with the mechanical drilling profile of the terrain. The surface layer, corresponding to topsoil and soil, is shown in green and presents intermediate resistivity values ($\approx 15 \Omega \text{ m}$). The resistivity areas (depicted in blue in the profile, $\approx 10 \Omega \text{ m}$) seen in this layer indicate the presence of moisture on the ground surface as tomography was performed during the rainy season. The high resistivity layer (in yellow and red, $\approx 24 \Omega \text{ m}$), identified at greater depths, suggests fresh bedrock. Finally, at the bottom, there is an additional low resistivity area (blue, $\approx 10 \Omega \text{ m}$) that indicates a high moisture content, meaning the probable presence of groundwater in the aquifer.

The variations in resistivity suggest the possibility of fractures in the bedrock, locating the contact between the two areas with contrasting resistivity at different depths. The most important appears as located at about 18–19 m along the profile, and other possible fractures are shown at 9 m and 33 m along the profile (Fig. 8).

Soil and rock physicochemical tests

Table 5 presents the results of the different physicochemical tests performed on the soil and rock at the site. K_2O remains almost stable in all layers (0.9 to 0.8%). Reactivity (pH) ranged from 8.2 in the topsoil to 7.6 in marlstone. Following the same trend with depth, the percentage of organic matter content lowered from 6.0 to 1.6, SiO_2 from 59.2 to 54.7, Al_2O_3 from 13.2 to 10.0, and Fe_2O_3 from 6.6 to 4.6. The following increased: CaCO_3 from 5.1 to 19.1%, SO_4^{2-} from < 0.02 to 0.28 mg/kg, SO_3 from 0.1 to 4.9%,

Table 3 Axial compression applied to rock cores

Hole	Sample	Depth (m)	q_u (kg/cm ²)	γ_m (kg/m ³)	v_s (m/s)	E_{av} (kg/cm ²)
H-1	Sample 4–1	6.40	151	2064	618	19 266
	Sample 4–2	7.60	161	2175	869	40 179
	Sample 4–3	9.80	185	2149	899	42 478

Table 4 Description of discontinuities

	Description	Spacing	Designation of rock mass
1. Discontinuity spacing	Spaced to widely spaced	0.60 to 2.00 m	Massive to solid
2. Condition of discontinuities	Roughness	Opening	Filling thickness
	Wavy smooth	Moderately open to closed	Very thin film
3. Designation of rock quality	From regular to excellent		
4. Persistence of discontinuities	Cannot be defined		
5. Orientation	Joints dive at different angles		
6. Presence of water in discontinuities	The fracture is dry, but there is evidence of flow circulation, such as stains and leaching		

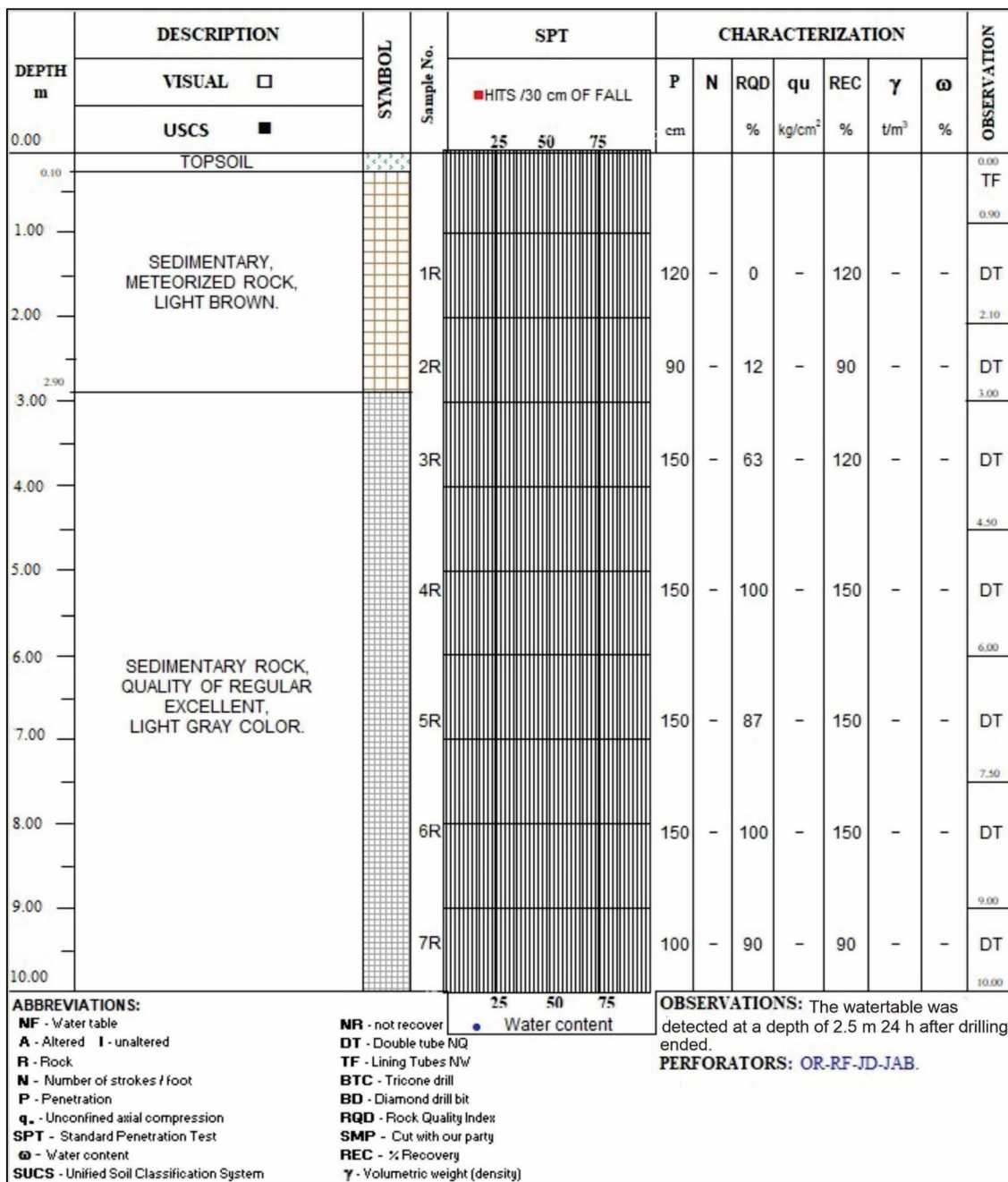


Fig. 5 Drilling profile of the drill hole

CEC from 24.3 to 46.2 meq/100 g, CaO content from 1.8 to 4.0%, MgO from 2.0 to 2.5% and Na₂O from 1.4 to 2.4%. The salts contents, as indicated by EC, also increases, from 0.2 to 2.2 dS/m, a difference that in the case of rocks is not significant: EC value of 2.2 dS/m may correspond to water in contact with a carbonate-rich rock, such as the studied one (11.8 to 19.1% CaCO₃). Furthermore, the CaO and MgO contents, which also increases at depth, justifies this increase in EC.

Discussion

Based on the results obtained for the geotechnical parameters, as well as a low resistivity zone identified, we have good indications of the presence of weathered rock and a water-saturated aquifer/water-filled rock, overlaid by residual soil with a lower-than-expected thickness for this region. In particular, soil extends to a 1-m depth and consists of a very thin “A”-type horizon that is very rich in

Fig. 6 Electrical resistivity tomography obtained using a smooth inversion of the least square optimization method. *w.t* watertable

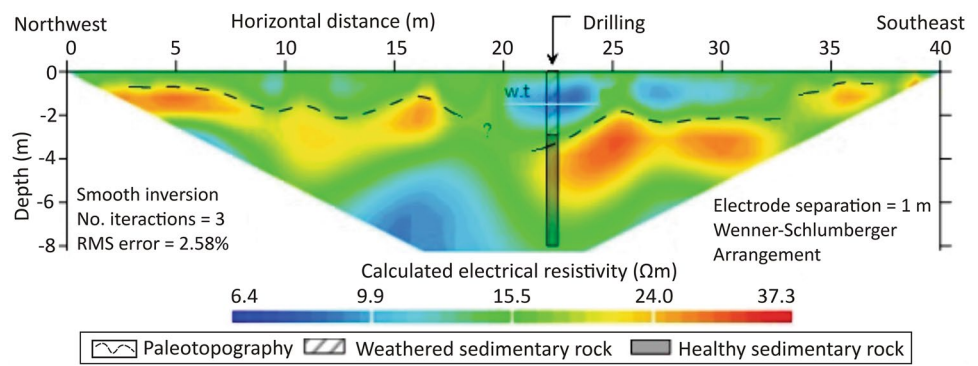


Fig. 7 Electrical resistivity tomography obtained using a robust inversion of the least squares' optimization method. *w.t* watertable

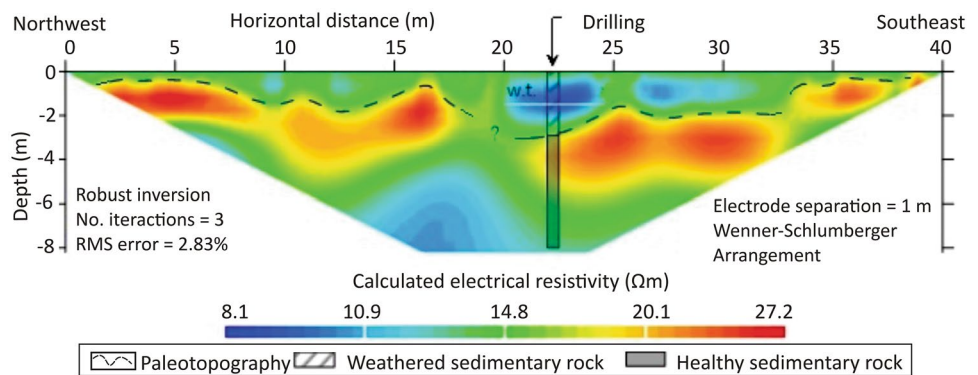
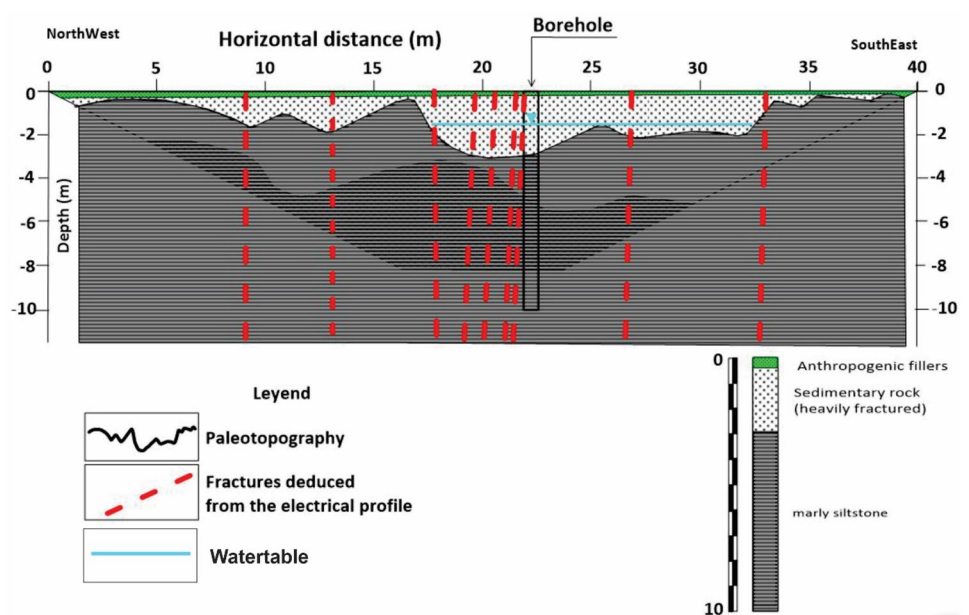


Fig. 8 Geological profile interpreted based on the lithology and fractures deduced from the electrical profile



organic matter, whereas the rest of the soil corresponds to a “C”-type horizon, with the marked presence of a gravel fraction. This AC soil is not at all characteristic of soils in areas characterized by a savanna tropical climate, where rainy weather favors much more complete soil profiles. Accordingly, soil can be interpreted as a technosol or

anthrosol, and possibly corresponds to a more complete soil partly dismantled by human activities in a residential/ industrial area (Ruiz et al. 2020). The study area corresponds to a type-C soil profile, which is dense soil and soft rock, as its cutoff velocity value (v_s) is 694 m/s.

Table 5 Physicochemical parameters and geochemical analysis for soil and rock

Parameters	Sample 1	Sample 2	Sample 3	Sample 4
pH	8.2	8.4	8.8	7.6
Electric conductivity (dS/m)	0.3	0.3	0.2	2.2
Organic matter content (%)	6.0	5.7	4.1	1.6
Calcium carbonate (%)	5.1	6.1	11.8	19.1
Sulfates (mg/kg)	< 0.02	< 0.02	< 0.02	0.28
Chlorides (mg/kg)	< 1.0	22.1	11.0	< 1.0
Cation exchange capacity (meq/100 g)	24.3	27.9	40.6	46.2
SiO ₂ (%)	59.2	58.9	57.4	54.7
Al ₂ O ₃ (%)	13.2	12.5	11.2	10.0
Fe ₂ O ₃ (%)	6.6	5.8	4.2	4.6
CaO (%)	1.8	2.5	3.5	4.0
MgO (%)	2.0	2.0	1.8	2.5
SO ₃ (%)	0.1	0.1	0.1	4.9
Na ₂ O (%)	1.4	1.4	1.4	2.4
K ₂ O (%)	0.9	0.8	0.9	0.8

The rest of the profile (1–10-m depth) is solid rock, constituted by marlstones with sedimentary stratification. It is possible to distinguish between the depth from 1 to 2.9 m, which corresponds to partly weathered rock, as evidenced by its light brown color (evidencing the preliminary formation of Fe oxyhydroxides), and the rest of the profile (2.9 to 10 m depth), where rock appears unweathered with the original grayish color. The discontinuities in both the weathered and healthy sedimentary rocks (marlstone; see Table 4) suggest that water circulates through them, which indicates rainwater infiltration through rocks and, thus, replenishes the aquifer (Arrocha 2015; Medici et al. 2016). The values for the axial compression not confined to the rock cores in subsamples 4 are similar to those reported in marl rocks from Saudi Arabia and Jordan (Shaqor et al. 2008; Mustafa et al. 2017).

In particular, the RQD values, together with the observational data for fracturation-related discontinuities (Table 4), indicate healthy rock with a very low degree of tectonic fracturation. In addition, the discontinuities in rock evidence water flow which, together with the lack of evident intergranular porosity and permeability, suggests that the aquifer is hosted in fractured rock (Healy & Cook 2002). The pumping test also evidences a semiconfined aquifer, as shown in the previous report by Vega (2004).

The electrical tomography profile interpretation allows us to deduce an irregular topography in contact between soil and rock substrate (Fig. 8). This topography, formed by grooves and peaks, is probably related to the fracturing observed in the test core. This character also allows us to suggest the presence of two aquifer types, both fractured. The upper aquifer, hosted in soil, corresponds to a free aquifer concentrated in areas with strongly fractured rocks and which, in turn, is delimited by some type of impermeable fracture. The lower aquifer corresponds to a semiconfined

aquifer, presents less fracturing and is delimited by fractures, such as those observed in the drilling profile. It is assumed to be in contact with the upper aquifer through some of these fractures.

Figure 9 illustrates an attempt made to correlate the results obtained from the geotechnical profile, the 2D electrical resistivity tomography and geochemistry, in the borehole. This figure presents the drilling profile at 10 m, together with variations in the calculated electrical resistivity and some geochemical parameters, such as CEC, % CaCO₃, pH and % organic content. We can see that the calculated electrical resistivity of subsoil decreases in the layer of clayey gravel and sedimentary rock to the watertable (1.5 m), and then increases at a depth of 4 m before lowering again at a depth of 8 m.

Soil and rock physicochemical tests indicate that reactivity (pH) varies between 7.4 and 8.5 in different layers, corresponding to moderately alkaline soils (Weaver et al. 1991). Thus, the organic layer, the clay gravel and healthy sedimentary rock had a moderate alkaline pH, while the weathered sedimentary rock had a marked alkaline pH greater than 8.5.

Based on the EC data (Clauser and Huenges 1995) we can interpretate the presence of two aquifers, the superficial and free one, and the lower one which should be semiconfined. On the other hand, both the borehole and the 2D tomography were carried out in the rainy season, which is consistent with the fact that we have a minimum EC at the upper level and an EC of 2.2 dS/m at the lower level, which indicates that in the upper part the salinity is more diluted due to the rapid recharge linked the seasonal rains, which would explain the slightly higher saline content at depth.

Organic matter content is, as expected, higher in the thin topsoil layer (6.0%) and lowers with depth. It takes a value of 5.7% in the “C” horizon and is much lower in rock (4.1%

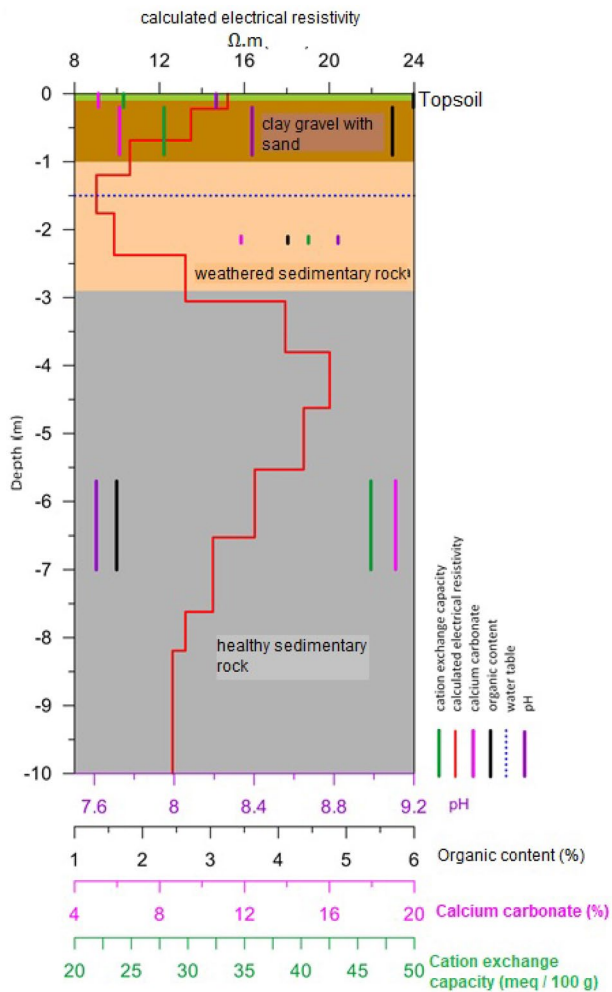


Fig. 9 Graphical representation of the stratigraphy of the profile, including values for the geochemistry and the determined electrical resistivity parameters, in the borehole

in the weathered sedimentary rock, possibly indicating some infiltration of colloidal organic matter from the overlying soil, and 1.6% in the healthy sedimentary rock).

The CaCO_3 content values increase with depth, with values of 5.1% for the organic layer, 11.8% for weathered rock and 19.1% for the healthy sedimentary rock. These values imply that this host rock is calcareous marlstone. However, it is not easy to determine whether the lower CaCO_3 content for the weathered rock corresponds to an original difference in composition, possibly in marlstone sequences (Derriche and Cheikh-Lounis 2004), or if this difference results from the higher degree of weathering at this level, which would imply the partial hydrolysis and washing of this component. In any case, the chemistry of the local groundwater, which is of the sodium bicarbonate type with HCO_3^- values in groundwater ranging from 215.40 and 278.85 mg/L (González-Valoys et al. 2021), clearly indicates the contribution of this lithology

to its composition, as indicated by other studies in waters obtained from marlstone (Wersin et al. 2016).

The first three layers have sulfate values below the detection limit (0.02 mg/kg) of the employed method, the value of the last layer being 0.28 mg/kg SO_4^{2-} . These are low values for this anion, which is usually low in marlstone lithology (Derriche and Cheikh-Lounis 2004). As expected, and in parallel to the sulfate values, % SO_3 is very low in the three most superficial samples and is higher in the deepest one. Groundwater has sulfate values of between 64.85 and 127.30 mg/L (González-Valoys et al. 2021) and, thus, suggests the dissolution of the sulfates contained in marls, could also contribute to higher EC electrical conductivities, as evidenced by another study about the waters obtained for this lithology (Wersin et al. 2016).

Chloride ions have the particularity of moving and dissolving in the soil profile according to runoff and precipitation (Custodio and Llamas 1976; Tan et al. 2017). The samples for this study were taken during the transition from the dry to the rainy season, and after the first rains had mobilized soluble salts to the second layer. The presence of this anion may be related to the influence of marine aerosols, which are deposited on topsoil and then filter down to, and are concentrated in, the “C” horizon, to act in this location as a proto- “B” horizon. Concentrations in the marlstone rock are lower than the unit, indicating that chloride salts are absent in the rock (Derriche and Cheikh-Lounis 2004). The chloride values in groundwater were between 11.20 and 22.37 mg/L (González-Valoys et al. 2021). In this case, marl rock does not provide chlorides, but allows chloride-containing water to infiltrate from the surface (Appelo and Postma 2004; Shomar 2015).

CEC is soil’s ability to retain and exchange different mineral elements. This parameter depends on the texture of soil and organic matter content (Weaver et al. 1991). The CEC values are 24.3 meq/100 g for sample 1, 27.9 meq/100 g for sample 2, 40.6 meq/100 g for sample 3 and 46.2 meq/100 g for sample 4, and are higher in rock. The interchangeable cations of the analyzed samples are likely to be K^+ , Ca^{2+} , Fe^{2+} , Na^+ and Al^{3+} (Custodio and Llamas 1976). The increase in CEC with depth explains the corresponding rise in % CaO, % Na_2O and % MgO, which are the main cations in the analyzed groundwater (González-Valoys et al. 2021; Armengol et al. 2017; Martínez et al. 2017). The soil fertility parameter corresponds to medium fertility soil (Vázquez and Bautista 1993), which is useful to know if it is to be used for cultivation and planting purposes.

The concentration of other metal oxides, such as SiO_2 , Al_2O_3 and Fe_2O_3 , lowers as depth increases. Indeed, their values lower with each layer. K_2O content remains low in all the layers as potassium is a minority cation in this type of sedimentary rock (Oke et al. 2017).

Conclusions

The studied profile corresponds to sections including a portion of soil, that are around 1 m in depth, and a marl-type rock which is much thicker than the drilled depth (10 m). Soil is probably a partial section of the original soil, and is likely to have been partially excavated and dismantled by human activities.

According to the edaphological characterization, the studied residual soil corresponds to technosol or anthrosol, and can be considered a permeable and transmissive level that favors rainwater infiltration, as confirmed by the good correspondence between rainfall and the water table rise. These characteristics also promote the infiltration of the chlorides present in soils as a result of transportation in marine aerosols from the nearby ocean. However, soil seems to act as a chemical barrier to this process by favoring the immobilization of this cation at this level.

The underlying sedimentary rock corresponds to a marl, particularly to marly siltstone, with a CaCO_3 content of 19.1%. It has a low, but measurable, content in sulfates, and a very low to null content in chlorides. Upon visual inspection, it is evident that the rock close to the soil–rock interface is weathered, as denoted by a brownish color indicative of the incipient oxidation of the Fe minerals present in rock. As also evidenced by the visual inspection, and confirmed by the RQD determinations, rock presents a certain degree of tectonic fracturation, which is likely to allow water to infiltrate and accumulate in rock, thus, constitute an aquifer.

The 2D electrical resistivity tomography confirmed the relevance of this technique for the study of the presence of water in soil and subsoil. In this case, the technique proved its ability to accurately identify the soil–rock interphase topography and was also able to suggest two water accumulations: one superficial, associated with the presence of water in soil, and a deeper one, related to the fractured aquifer. This technique correctly identifies areas with higher fracturation ratios, which may be interesting for the detailed research of favorable sites for deeper drilling to obtain bigger water reserve volumes.

A good agreement appears between the chemistry of water, as characterized in a previous study, and that of the rock studied in the drill section, especially as regards the presence of carbonates and sulfates an, alkaline pH, and medium to high CEC. These characteristics make local water suitable for use for irrigation and as a source of drinking water.

Based on our results, we recommend a more complete study of the possibilities of water production in this area, which would include the more extensive use of electrical

tomography, such as increase the spread (either profile length, electrode spacing, or number of electrodes) to image deeper to better characterize the deeper aquifer, as well to find the most favorable areas, characterized by higher tectonic fracturation. Other elements to bear in mind during this study would be to avoid proximity to the coast so that the infiltration of chlorides from marine aerosols would be minimized. The water chemistry should also be the subject of further studies, including the characterization of potential pollutants related to human activities, given the area's proximity to industrial and residential areas.

Acknowledgements The authors thank the Technological University of Panama for its collaboration during this research work, the Centro de Investigaciones Hidráulicas e Hidrotécnicas (CIHH), the Centro Experimental de Ingeniería (CEI) and its laboratories, the Laboratorio de Geotecnia (LABGEO), the Laboratorio de Investigación en Ingeniería y Ciencias Aplicadas (LIICA) and the Laboratorio de Análisis Industriales y Ciencias Ambientales (LABAICA). We also thank CEMEX Panama for collaborating with the X-ray fluorescence determinations, and the human team in each laboratory, especially David Vega, Dr. Alexis Mojica, Dr. Cecilio Hernández, Fidedigna de Ortiz, José Pérez and Ana Franco. The Secretaría Nacional de Ciencia, Tecnología e Innovación (SENACYT) and the Instituto para la Formación y Aprovechamiento de Recursos Humanos (IFARHU) of Panama, the Sistema Nacional de Investigación de Panamá (SNI), and the University of Castilla-La Mancha (UCLM), the University of Oviedo and the Autonomous University of Madrid (UAM) are also thanked for supporting this research. Thanks also go to Andrew Frankland (Scientific English) and Helen Warburton (Scientific English) for revising the English style of the manuscript.

Author contributions The paper was written by AGV, MVL, EG, JA, EGO, PC, FJGN, RJB and PH. The physico-chemical soils and rock samples were processed and analyzed by AGV. Geotechnical tests were performed by JA and petrography by EG.

Funding Open Access funding provided thanks to the CRUE-CSIC agreement with Springer Nature. This study was funded by the Secretaría Nacional de Ciencia, Tecnología e Innovación (SENACYT), the Instituto para la Formación y Aprovechamiento del Recurso Humano (IFARHU) of Panama (270-2019-109), and Fondos para Grupos de Investigación UCLM (2020-GRIN-27011).

Declarations

Conflicts of interest The authors declare no conflict of interest.

Availability of data and materials Not applicable.

Code availability Not applicable.

Animal research Not applicable.

Ethics approval Not applicable.

Consent to participate Not applicable.

Consent for publication Not applicable.

Open Access This article is licensed under a Creative Commons Attribution 4.0 International License, which permits use, sharing, adaptation, distribution and reproduction in any medium or format, as long as you give appropriate credit to the original author(s) and the source, provide a link to the Creative Commons licence, and indicate if changes were made. The images or other third party material in this article are included in the article's Creative Commons licence, unless indicated otherwise in a credit line to the material. If material is not included in the article's Creative Commons licence and your intended use is not permitted by statutory regulation or exceeds the permitted use, you will need to obtain permission directly from the copyright holder. To view a copy of this licence, visit <http://creativecommons.org/licenses/by/4.0/>.

References

- AASHTO T 291 (2013) Standard method of test for determining water-soluble chloride ion content in soil Single User Digital Publication. American Association of State Highway and Transportation Officials
- Abdel-Satar A, Al-Khabbas M, Alahmad W, Yousef W, Alsomadi R (2017) Quality assessment of groundwater and agricultural soil in Hail region, Saudi Arabia. *Egypt J Aquat Res* 43:55–64. <https://doi.org/10.1016/j.ejar.2016.12.004>
- Abiye T, Masindi K, Mengistu H, Demlie M (2018) Understanding the groundwater-level fluctuations for better management of groundwater resource: a case in the Johannesburg region. *Groundw Sustain Dev* 7:1–7. <https://doi.org/10.1016/j.gsd.2018.02.004>
- Alpirez J, Aviles K, Chiari K, Chung Y, Pinzón I, Samudio M, Vega D (2015) Proyecto de Agua Subterránea, Acuífero de la UTP, Extensión Tocumen. pp 1–19.
- Appelo C, Postma D (2004) *Geochemistry, groundwater and pollution*, 2nd Edition. CRC press, Boca Raton. ISBN 0415364213, pp 1–649.
- Armengol S, Manzano M, Bea S, Martínez S (2017) Identifying and quantifying geochemical and mixing processes in the Matanza-Riachuelo Aquifer System, Argentina. *Sci Total Environ* 599–600:1417–1432. <https://doi.org/10.1016/j.scitotenv.2017.05.046>
- Arrocha J (2015) Informe sobre Ensayos Geotécnicos para el Estudio Hidrogeoquímico de las Aguas Subterráneas del Pozo Ubicado en la Extensión Tocumen, Universidad Tecnológica de Panamá; para la tesis de la Lic. Ana González (Panamá, Tocumen: Universidad Tecnológica de Panamá, Centro Experimental de Ingeniería, Laboratorio de Geotecnia), pp 1–24.
- ASTM (2004) Volume 04-09. In *Annual Book of ASTM Standards*. International Standard World Wide, American Society Testing of Materials (ASTM). Section four, Constructions Volume 04.08 and 04.09, Soil and Rock (I). C6913, D1580. D2487, D2974, D4318, D4972, D7012.
- Bakhsipour Z, Asadi A, Huat B, Sridharan A, Kawasaki S (2016) Effect of acid rain on geotechnical properties of residual soils. *Soils Found* 56:1008–1020. <https://doi.org/10.1016/j.sandf.2016.11.006>
- Barberá J, Jódar J, Custodio E, González-Ramón A, Jiménez-Gavilán P, Vadillo I, Pedrera A, Martos-Rosillo S (2018) Groundwater dynamics in a hydrologically-modified alpine watershed from an ancient managed recharge system (Sierra Nevada National Park, Southern Spain): insights from hydrogeochemical and isotopic information. *Sci Total Environ* 640–641:874–893. <https://doi.org/10.1016/j.scitotenv.2018.05.305>
- Benabdelouhab S, Salhi A, Himi M, Stitou El Messari J, Casas Ponsati A, Mesmoudi H, Benabdefadel A (2018) Using resistivity methods to characterize the geometry and assess groundwater vulnerability of a Moroccan coastal aquifer. *Groundw Sustain Dev* 7:293–304. <https://doi.org/10.1016/j.gsd.2018.07.004>
- Centro de Investigaciones Hidráulicas e Hidrotécnicas (2016) Data de niveles piezométricos del pozo de la Extensión Tocumen, Universidad Tecnológica de Panamá, pp 1–24.
- Chidya R, Matamula S, Nakoma O, Chawinga C (2015) Evaluation of groundwater quality in rural-areas of northern Malawi: case of zombwe extension planning area in Mzimba. *Phys Chem Earth* 93:55–62. <https://doi.org/10.1016/j.pce.2016.03.013>
- Clauser C, Huenges E (1995) Thermal conductivity of rocks and minerals. *Rock Phys Phase Relat* 3:105–126
- Contraloría General de la República de Panamá (2010) Retrieved 10th March 2021 from: <http://www.contraloria.gob.pa/inec/archivos/P3551P3551cuadro3-08.xls>
- Custodio E, Llamas M (1976) *Hidrología Subterránea*. Ediciones Omega, Barcelona, Spain. Tomo I y II, ISBN 8428204462 obra completa, pp 1–2418.
- De Caro M, Crosta G, Frattini P (2017) Hydrogeochemical characterization and Natural Background Levels in urbanized areas: Milan Metropolitan area (Northern Italy). *J Hydrol* 547:455–473. <https://doi.org/10.1016/j.jhydrol.2017.02.025>
- Derriche Z, Cheikh-Lounis G (2004) Geotechnical characteristics of the Plaisancian marls of Algiers. *Bull Eng Geol Env* 63:367–378. <https://doi.org/10.1007/s10064-004-0246-5>
- Diario De Las Américas (2020) Sequía amenaza con cierre del Canal de Panamá. Retrieved 13 August 2021, from: <https://www.diariolasamericas.com/economia/sequia-amenaza-cierre-del-canal-panama-n4206501>
- Dirección de Hidrometeorología de ETESA (2007) Mapa de Clasificación Climática (según Köppen). Retrieved May 23, 2020 from <http://www.hidromet.com.pa/mapas.php>
- Dirección de Hidrometeorología de ETESA (2021) ETESA Hidrometeorología, datos diarios. Retrieved March 21, 2021 from <https://www.hidromet.com.pa/es/datos-diarios>
- El País (2020) Sequías o agua en tromba: el clima ya desestabiliza el canal de Panamá. Retrieved 13 August 2021, from: <https://elpais.com/sociedad/2020-08-17/el-cambio-climatico-acechal-canal-de-panama.html>
- González-Valoys A, Vargas-Lombardo M, Higuera P, García-Navarro F, García-Ordiales E, Jiménez-Ballesta R (2021) Hydrochemistry of groundwater from Tocumen sector, Panama city: an assessment of its possible usage during emergency events. *Environ Earth Sci* 80:176. <https://doi.org/10.1007/s12665-021-09497-7>
- Guardia (2018) *Geology of the Republic of Panama - Feature Layer*. Retrieved 15 November 2019, from: <https://www.arcgis.com/apps/mapviewer/index.html?layers=343419d1aca4452585e47eb7f4d012de>
- Gutiérrez E (2021) Informe petrográfico de la roca del acuífero de la Extensión UTP Tocumen, para la Lic. Ana González, pp 1–2.
- Healy R, Cook P (2002) Using groundwater level to estimate recharge. *Hydrogeol J* 10:91–109. <https://doi.org/10.1007/s10040-001-0178-0>
- Ho C, Mojica A, Pinzón R, Díaz I, Llubes M (2017) Non-invasive time-lapse imaging of rainfall infiltration levels in the sedimentary soils of central Panama. *Sustain Environ*. <https://doi.org/10.22158/se.v2n2p148>
- Jordanova D, Goddu S, Kotsev T, Jordanova N (2013) Industrial contamination of alluvial soils near Fe-Pb mining site revealed by magnetic and geochemical studies. *Geoderma* 192:237–248. <https://doi.org/10.1016/j.geoderma.2012.07.004>
- Kiamco C, Alfaro C, Asensio E, Berman G, Calvo A, DePuy M, Franco O, Franceschi P, Guerra F, García L, Hassel, A, Isaac M, Ng E, Ramírez U, Ulloa D, Yinh J (2004) Reglamento de Diseño Estructural para la República de Panamá-2004, pp 1–267.

- Kruseman G, De Ridder N, Verweij J (1970) Analysis and evaluation of pumping test data. International Institute for Land Reclamation and Improvement, The Netherlands, pp 1–200
- Kumar D, Mondal S, Nandan MJ et al (2016) (2016) Two-dimensional electrical resistivity tomography (ERT) and time-domain-induced polarization (TDIP) study in hard rock for groundwater investigation: a case study at Choutuppal Telangana. *India Arab J Geosci* 9:355. <https://doi.org/10.1007/s12517-016-2382-1>
- La Estrella de Panamá, Panamá (2012) Vuelven las dudas por la planta de Chilibre. La Estrella de Panamá. Retrieved 15 November 2019, from: <https://www.laestrella.com.pa/nacional/121130/dudas-planta-vuelven-chilibre>.
- Martinez J, Raiber M, Cendon D (2017) Using 3D geological modelling and geochemical mixing models to characterise alluvial aquifer recharge sources in the upper Condamine River catchment, Queensland, Australia. *Sci Total Environ* 574:1–18. <https://doi.org/10.1016/j.scitotenv.2016.09.029>
- Medici G, West L, Mountney N (2016) Characterizing flow pathways in a sandstone aquifer: tectonic vs sedimentary heterogeneities. *J Contam Hydrol* 194:36–58. <https://doi.org/10.1016/j.jconhyd.2016.09.008>
- Mojica A, Díaz I, Ho C, Ogden F, Pinzón R, Fábrega J, Vega D, Hendrick J (2013) Study of seasonal rainfall infiltration via time-lapse surface electrical resistivity tomography: case study of Gamboa area, Panama Canal Watershed. *Air Soil Water Res* 2013(6):131–139. <https://doi.org/10.4137/ASWR.S12306>
- Mojica A, Solís J, Ortiz F, Duarte B, Harris J, Pastor L (2012) Detección de aguas subterráneas en los suelos sedimentarios de la Extensión de Investigación de Tocumen de la Universidad Tecnológica de Panamá mediante la imaginería bidimensional de resistividad eléctrica y refracción sísmica durante la época seca. *I+D Tecnológico*, 8(2), 5–14, ISSN: 1680–8894
- Mojica A (2015) Informe de Tomografía de Resistividad Eléctrica 2 D, Estudio hidrogeológico de las aguas subterráneas del pozo ubicado en el Campus de Investigación de Tocumen UTP, para la tesis de la Lic. Ana González. Panamá, Tocumen: Universidad Tecnológica de Panamá, Centro Experimental de Ingeniería, Laboratorio de Investigación en Ingeniería y Ciencias Aplicada, informe No.: CEI-07-SI-115–2015, pp 1–24.
- Mojica A (2018) Geoelectrical sounding and imaging over the central zone of Panama. *Intech*, Chapter 8, pp 137–144, <http://dx.doi.org/https://doi.org/10.5772/intechopen.74210>. Retrieved 12 February 2021 from: <http://www.intechopen.com/books/trends-in-telecommunications-technologies/gps-total-electron-content-tec-prediction-at-ionosphere-layer-over-the-equatorial-region%0AInTec>.
- Mustafa Y, Al-Hashemi H, Bukhary A (2017) Characterisation and index properties correlations for marlstone and marly limestone of Saudi Arabia. 2nd World Congress on Civil, Structural, and Environmental Engineering (CSEE'17), Paper No. ICGRE 104, ISSN: 2371–5294, DOI:<https://doi.org/10.11159/icgre17.104>
- Oke S, Vermeulen D, Gomo M (2017) Intrinsic vulnerability assessment of shallow aquifers of the sedimentary basin of southwestern Nigeria. *Jamba J Disas Risk Stud* 10(1):a333. <https://doi.org/10.4102/jamba.v10i1.333>
- Ruiz F, Perlatti F, Oliveira DP (2020) Revealing tropical technosols as an alternative for mine reclamation and waste management. *Minerals* 10:110. <https://doi.org/10.3390/min10020110>
- Shaour F, Jarrar G, Hencher S, Kuisi M (2008) Geotechnical and mineralogical characteristics of marl deposits in Jordan. *Environ Geol* 55:1777–1783. <https://doi.org/10.1007/s00254-007-1128-5>
- Shomar B (2015) Geochemistry of soil and groundwater in arid regions: Qatar as a case study. *Groundw Sustain Dev* 1:33–40. <https://doi.org/10.1016/j.gsd.2015.12.005>
- Skinner S, Halstead R (1958) Note on rapid method for determination of carbonates in soils. *Can J Soil Sci* 38(2):189–190
- Tan H, Liu Z, Rao W, Wei H, Zhang Y, Jin B (2017) Stable isotopes of soil water: implications for soil water and shallow groundwater recharge in hill and gully regions of the Loess Plateau, China. *Agr Ecosyst Environ* 243:1–9. <https://doi.org/10.1016/j.agee.2017.04.001>
- The Constructor (2018) What is RQD (Rock Quality Designation)? Retrieved March 2021 from: <https://theconstructor.org/geotechnical/rqd-rock-quality-designation-calculation/20536/>.
- Vázquez A, Bautista N (1993) Guía para interpretar el análisis químico de suelo y agua. Departamento de Suelos, Universidad Autónoma de Chapingo, México, N° folleto 1049, pp 1–29.
- Vega D (2004) Informe de Prueba de Bombeo, Pozo de Extensión Tocumen, Centro de Investigaciones Hidráulicas, pp 1–10.
- Wahab S, Saibi H, Mizunaga H (2021) Groundwater aquifer detection using the electrical resistivity method at Ito Campus, Kyushu University (Fukuoka, Japan). *Geosci Lett* 8:15. <https://doi.org/10.1186/s40562-021-00188-6>
- Weaver R, Syers J, Jackson M (1991) Análisis Químico de Suelos. Ed. Omega (Madrid), ISBN: 978-8428201438. pp 267
- Wersin P, Mazurek M, Mäder U, Gimmi T, Rufer D, Lerouge C, Traber D (2016) Constraining porewater chemistry in a 250 m thick argillaceous rock sequence. *Chem Geol* 434(2016):43–61. <https://doi.org/10.1016/j.chemgeo.2016.04.006>
- Zhang X, Hu B, Wang P, Chen J, Yang L, Xiao K (2018) Hydrogeochemical evolution and heavy metal contamination in groundwater of a reclaimed land on Zhoushan island. *Water* 10(3):316. <https://doi.org/10.3390/w10030316>

Publisher's Note Springer Nature remains neutral with regard to jurisdictional claims in published maps and institutional affiliations.